International Journal for Housing Science and Its Applications
Publish August 10, 2025. Volume 46, Issue 4 Pages 4378-4392

https://doi.org/10.70517/ijhsa464284

Research on Optimizing the Automatic Load Regulation of Virtual Power Plants Using Fuzzy Logic Algorithm under the Framework of Electronic Scale

Wenshao Li[1], Baolu Wang[1], Guipin He[1], Hongyuan Liu[1], Paiyi Li[1] and Wei Liu[2,*]
[1] Liuzhou Cigarette Factory, Tobacco Guangxi Industrial Co., Ltd., Liuzhou, Guangxi, 545005, China
[2] School of Civil Engineering, University of South China, Hengyang, Hunan, 421001, China
Corresponding authors: (e-mail: CNLiu8544@163.com).

Abstract Virtual power plant (VPP) can effectively integrate geographically dispersed and different types of distributed new energy and customer loads on a large scale, break the boundaries between the generation side and the load side, and improve the reliability of power supply, which is an important means to solve the problem of new energy into the grid. The study first constructed a virtual power plant model within the framework of an electronic scale, takes the minimization of VPP operation cost as the objective function, establishes an economic optimization scheduling model of VPP considering the load of the virtual power plant, and searches for the optimal value of the objective function to realize the economic operation of the virtual power plant by using the HGWO algorithm. The simulation results show that the HGWO algorithm can achieve high economic efficiency and high reliability compared with the GWO method. The fine classification of loads to participate in demand response maximizes the benefits of the virtual power plant in the electricity market, minimizes the peak-to-valley difference in the user curve, and minimizes the user cost.

Index Terms virtual power plant, electronic scale, hybrid gray wolf algorithm, load balancing

I. Introduction

Under the guidance of the “dual-carbon” goal, the installed capacity and power generation of new energy sources, represented by wind power and photovoltaic (PV), have been rising year by year, promoting the clean and green transformation of traditional energy sources. However, with a high proportion of new energy access and peak hour power demand growth, China's power supply and demand balance pressure is increasing, only source-side regulation is difficult to ensure the economic and stable operation of power, significantly increasing the planning and operation costs of the power system [1]-[3]. It is necessary to scientifically assess and accurately regulate the demand-side resources, deeply excavate the potential of demand-side resource regulation, so that it can play the same role as the power-side resources, realize the efficient use of energy, and strongly support the power supply and renewable energy consumption [4]-[6].

With the gradual development of power plants in the direction of automation, bidding for Internet access and plant-network separation have become the focus of research. Improve the unit operation safety, and the reasonable allocation of the unit, so as to reduce the energy consumption of power generation and promote the development of modern market economy [7]. Therefore, the virtual power plant and information technology can be used to make a single uncontrollable idle load accumulation, so as to constitute a controllable power supply and demand network, so that the precise regulation of the network load research has an important role [8]-[10]. Virtual power plant is a kind of power coordination management system through advanced information and communication technology and software system, to realize the aggregation and coordination optimization of distributed power supply, energy storage system, controllable load, electric vehicles and other energy sources, in order to participate in the power market and grid operation as a special power plant [11]. At the same time, it is also a source-network-load aggregation management model under the “Internet +” intelligent energy environment, with the user as the center and the commercialized market as the platform [12]. At this stage, relevant intelligent technologies can be used to build an online measurement and evaluation index system for load regulation potential, to help virtual power plant operators grasp the actual adjustable potential of existing user resources, and to provide reliable data support for virtual power plant operators to participate in the declaration of electric power demand response projects, and to respond to the volume and price of the response [13]-[16].

The study constructs the basic structure of the virtual power plant containing renewable energy units, conventional thermal power units, and energy storage devices, and models the virtual power plant. Secondly, a fuzzy chance

constraint algorithm is introduced to deal with the uncertainty of wind power output and load. Minimizing the operating cost of VPP is taken as the objective function, and various kinds of constraints existed in the operation process of VPP are taken into consideration, and an economic dispatch model of VPP based on the hybrid gray wolf (HGWO) algorithm is constructed. A load optimization scheduling method is designed for optimal scheduling analysis, and the load is refined to participate in demand response, and a comparative analysis is carried out in four scenarios from the state of the VPP energy storage device, the load profile, the cost of electricity consumption of the customer, and the unbalanced output of the VPP.

II. Fuzzy logic based virtual power plant modeling and its uncertainty

II. A. Virtual power plant structure

Virtual power plants are usually based on advanced technologies such as data exchange and data communication, integrating and optimizing different types of power generation units, realizing the coordinated operation of each unit through a higher level of software architecture, and then participating in the power market or auxiliary services. Virtual power plant is essentially a large-scale system that can realize the coordination and cooperation between resources, and its operation mode is very similar to that of conventional power plants. The virtual power plant proposed in this paper adopts a centralized control method, and its basic structure is shown in Figure 1.

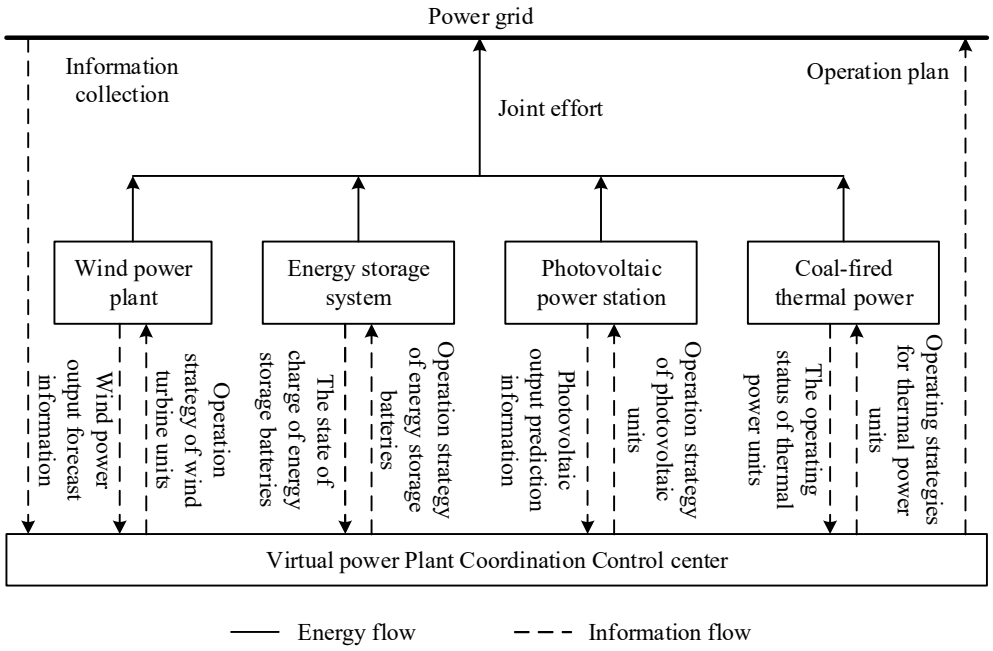

Figure 1: Basic structure of virtual power plant

As can be seen from the figure, the virtual power plant is connected to the power grid through the control center, which comprehensively collects and integrates the relevant information of the subordinate units according to the information collection and communication network, coordinates and regulates the utilization of resources, and finally cooperates with the power grid to participate in the scheduling, which provides important support for the stable operation of the virtual power plant and the power grid. The virtual power plant in this paper consists of a wind farm, a photovoltaic power plant, a coal-fired thermal power plant, and an energy storage system.

II. B. Modeling of the units of the virtual power plant

II. B. 1) Wind turbine modeling

Wind has kinetic energy, by driving the fan blade rotation, the kinetic energy of the wind is first converted into the mechanical energy of the blade, and then through the generator is converted into electrical energy. However, the wind speed will be affected by weather, environment, geographic location and other factors, and due to the uneven heating of the ground surface, different regions of the absorbed solar radiation energy is different, resulting in the wind speed has a random character, then the fan output power also shows a significant randomness. The wind speed probability density function can be expressed as:

$$f(v)=\frac{k}{c}\left(\frac{v}{c}\right)^{k-1}e^{-\left(\frac{v}{c}\right)^{k}} \tag{1}$$

Here, v is the actual wind speed; k is the shape parameter; and c is the scale parameter.

If the mean and variance of wind speed are known, k and c can be found:

$$k=\left(\frac{\sigma_w}{\overline{v}}\right)^{-1.086},1\le k\le 10 \tag{2}$$

$$c=\frac{\overline{v}}{\tau\left(1+\frac{1}{k}\right)} \tag{3}$$

Here, $\overline{v}$ is the mean value of wind speed; σ_w is the standard deviation of wind speed; τ is the Gamma function.

The output power of the wind turbine usually follows the following law: if the actual wind speed is lower than the cut-in wind speed or higher than the cut-out wind speed, the output power is zero: if the wind speed is between the cut-in wind speed and the rated wind speed, the output power is linear with the wind speed; if the wind speed is between the rated wind speed and the cut-out wind speed, the output power is constant as the rated output power. That is:

$$P_w=\begin{cases}0 & v<v_{in},v>v_{out}\\ P_E\cdot\dfrac{v-v_{in}}{v_e-v_{in}} & v_{in}\le v\le v_e\\ P_E & v_e\le v\le v_{out}\end{cases} \tag{4}$$

Here, P_w is the actual output power; P_E is the rated output power; v_{im},v_{out},v_e are the wind turbine's cut-in, cut-out and rated wind speeds, respectively.

II. B. 2) Modeling of photovoltaic units

Distributed PV is not only constrained by environmental conditions such as geographic location, seasonal n weather and operational conditions such as light conditions, but also by neighboring PV units and connected power loads. It is usually considered that the PV unit output is proportional to its light intensity and obeys the Beta distribution.

First, the light intensity is standardized:

$$I_0=\frac{I_i}{I_{\max}} \tag{5}$$

Here, I_t is the actual illumination; $I_{\max}$ is the illumination maximum.

The probability density and probability distribution of illumination are as follows:

$$f(I_0)=\frac{\Gamma(\alpha+\beta)}{\Gamma(\alpha)\Gamma(\beta)}(I_0)^{\alpha-1}(1-I_0)^{\beta-1} \tag{6}$$

$$F(I_0)=\int_{I_1}^{I_2}f(I_0)dI_0 \tag{7}$$

Here, α and β are the shape parameters of the Beta distribution; I_1,I_2 are the lower and upper limits of the normalized illuminance.

Based on the historical data of illuminance, the sample mean μ_{pv} and standard deviation σ_{pv} can be derived, and the parameters of the Beta distribution can be obtained by further calculation.

$$\beta=(1-\mu_{pv})\left[\frac{\mu_{pv}(1+\mu_{pv})}{\sigma_{pv}^2}-1\right] \tag{8}$$

$$\alpha=\frac{\mu_{pv}\beta}{1-\mu_{pv}} \tag{9}$$

$$P_{pv} = S_{pv}\tau_{pv}I \tag{10}$$

II. B. 3) Energy storage system modeling

Adding an energy storage system to a virtual power plant can improve the consumption of renewable energy and smooth out the power. The energy storage system converts electrical energy into chemical energy, potential energy and other forms of energy for storage when charging, and then converts it into electrical energy when discharging. Currently common energy storage methods, chemical energy storage such as lead-acid batteries, sodium-sulfur batteries, etc. are more widely used. In this section, the charging and discharging state constraints, charging and discharging power constraints, and charging state constraints of the energy storage battery are modeled.

II. C. Uncertainty in virtual power plants

II. C. 1) Fuzzy chance constraints

Usually in optimization problems, for constraints containing fuzzy parameters, they can be formulated as:

$$\min f(x) \tag{11}$$

$$s.t.g(x,\varpi) \le 0 \tag{12}$$

Eq:

$f(x)$ - objective function; x - vector of decision variables; $g(x,\varpi)$ - constraints containing fuzzy variables; ϖ - vector of fuzzy variables.

In the process of scheduling model solution, the fuzzy parameters contained in the constraints will cause the model to be difficult to give a deterministic solution, which can be appropriately processed so that the constraints are established with a certain level of confidence α, denoted as:

$$Cr\left\{g(x,\varpi) \le 0\right\} \ge \alpha \tag{13}$$

Here, $Cr\{\}$ - credibility of events in $\{\cdot\}$.

II. C. 2) Clear equivalence classes for fuzzy parameters

When the constraint function $g(x,\varpi)$ has the following form:

$$g(x,\varpi) = h_1(x)\varpi_1 + h_2(x)\varpi_2 + \cdots + h_t(x)\varpi_t + h_0(x) \tag{14}$$

Here, $h_k(x)$ - a function containing only decision vectors; ϖ_k - fuzzy variables.

Define the following two functions:

$$h_k^+(x) = \begin{cases} h_k(x), h_k(x) \ge 0 \\ 0, h_k(x) < 0 \end{cases} \tag{15}$$

$$h_k^-(x) = \begin{cases} 0, h_k(x) \ge 0 \\ -h_k(x), h_k(x) < 0 \end{cases} \tag{16}$$

Specifically, when $h_k(x) = 1$, $h_k^+(x) = 1, h_k^-(x) = 0$; when $h_k(x) = -1$, $h_k^+(x) = 0, h_k^-(x) = 1$. If the confidence level $\alpha > 0.5$, the clear equivalence class of fuzzy constraints can be expressed as:

$$\begin{aligned} &(2-2\alpha)\sum_{k=1}^{l}\left[r_{k3}h_k^+(x) - r_{k2}h_k^-(x)\right] \\ &+(2\alpha-1)\sum_{k=1}^{l}\left[r_{k4}h_k^+(x) - r_{k1}h_k^-(x)\right] + h_0(x) \le 0 \end{aligned} \tag{17}$$

Here, $r_{k1} \sim r_{k4}$ - the affiliation parameter of the fuzzy variable ϖ_k, Here,

$$k = 1,2,\cdots,t, t \in R \tag{18}$$

In summary, the solution of optimization problems containing fuzzy parameters can be achieved by clear equivalence classes of fuzzy parameters.

II. C. 3) Affinity functions for fuzzy parameters

In this paper, the trapezoidal subordination function is used to describe each uncertainty quantity:

$$\mu(P_x)=\begin{cases}\dfrac{P_{x4}-P_x}{P_{x4}-P_{x3}} & P_{x3}<P_x\le P_{x4}\\ 1 & P_{x2}<P_x\le P_{x3}\\ \dfrac{P_x-P_{x1}}{P_{x2}-P_{x1}} & P_{x1}<P_x\le P_{x2}\\ 0 & \text{other}\end{cases} \tag{19}$$

$$P_{xn}=\omega_n P_{x,fc} \tag{20}$$

Here, $\mu(P_x)$ - the trapezoidal affiliation function of P_x; $P_{x1}\sim P_{x4}$ - the parameters in the trapezoidal affiliation function that determines the shape of the affiliation function, where P_{x1},P_{x4} are the upper and lower ranges of the parameter, and P_{x2},P_{x3} are the most probable values of the parameter; $P_{x,fe}$ - P_x is the predicted value, MW; ω_n - scale factor, usually determined from historical data on scenery and loads.

III. Virtual power plant load auto-regulation model

III. A. Virtual power plant load optimization scheduling model

III. A. 1) Objective function

In order to guarantee the economy of power plant operation and ensure the safe operation of the power system, the optimal scheduling model established in this paper chooses to minimize the operating cost of the virtual power plant as the objective function.

During the operation of the virtual power plant, the operation and maintenance costs of wind power, photovoltaic, thermal power, and energy storage batteries need to be considered comprehensively:

$$\min f=C_w+C_{pv}+C_{th}+C_{ES}+C_p \tag{21}$$

Here, C_w - wind power O&M cost, yuan; C_{pw} - photovoltaic O&M cost, yuan; C_{th} - - conventional thermal power unit generation cost, yuan; C_{ES} - energy storage battery O&M cost, yuan; C_p - new energy abandonment penalty cost, yuan.

III. A. 2) Stepped carbon transaction cost modeling

In order to promote the clean and low-carbonization of the power system, this paper combines the carbon trading mechanism and introduces the carbon trading cost into the total cost of the virtual power plant. In order to better control the carbon emissions of the system, the paper meters the step-type carbon trading cost model, compared with the traditional carbon trading. Introducing the scheduling model of step-type carbon trading will increase the difficulty of algorithm solving, making the solving time increase greatly. The stepped carbon trading cost model is:

$$C_{carbon}=\begin{cases}\lambda_c(M_{total}-M_{rate}), & M_{total}\le M_{rate}+d\\ \lambda_c d+(1+r)\lambda_c(M_{total}-M_{rate}-d), & \\ M_{rate}+d<M_{total}<M_{rate}+2d & \\ (2+r)\lambda_c d+(1+2r)\lambda_c(M_{total}-M_{rate}-2d), & \\ M_{total}\ge M_{mte}+2d & \end{cases} \tag{22}$$

Here, λ_c --initial carbon trading price, yuan; M_{total} --total carbon emissions of the virtual power plant, t; M_{rate} - Initially given carbon emission quota of the virtual power plant, t; d - Carbon emission interval length; r - Carbon emission per step up of the carbon trading price increase.

Wind and solar energy are clean energy sources that produce almost no carbon emissions in the power generation process, thus coal-fired thermal power units are used as the source of carbon emissions in the virtual power plant. The model that carbon emissions from thermal power units are proportional to output power is used, i.e.:

$$M_{total}=\sum_{j=1}^{M}\sum_{i=1}^{N}\varphi_{th,j}P_{th,j}(i) \tag{23}$$

Here, φ_{thj} - carbon emissions per unit output power of the j th coal-fired thermal power unit, t/MW.

In summary, with the addition of carbon trading costs to the original costs, there is an objective function:

$$\min f=C_w+C_{pv}+C_{th}+C_{ES}+C_p+C_{carbon} \tag{24}$$

III. A. 3) Constraints

(1) System power balance constraints

$$P_w(i)+P_{pv}(i)+\sum_{j=1}^{M}P_{th,j}(i)+P_{ES}(i)=P_{load}(i) \tag{25}$$

Here, $P_{ES}(i)$ - the power of the energy storage battery at the i moment, MW.

(2) Thermal power unit output constraint

$$P_{th,j,\min}\le P_{th,j}(i)\le P_{th,j,\max} \tag{26}$$

Here, $r_{up,j}, r_{down,j}$ - the maximum upward and downward climbing power of the j th thermal power unit, MW/h.

(3) Climbing constraints for thermal power units

$$-r_{down}\cdot\Delta t\le P_{th,j}(i+1)-P_{th,j}(i)\le r_{up}\cdot\Delta t \tag{27}$$

Here, $r_{up,j}, r_{down,j}$ - the maximum upward and downward climbing power of the j th thermal power unit, MW/h; Δt - the time interval s between two sampling points.

III. B. Handling of wind and load uncertainty

Processing the power balance constraints, rotating standby constraints in the scheduling model, even if they all hold at confidence level α, the credible chance constraints on the power balance of the system can be expressed as follows:

$$Cr\left\{\tilde{P}_{load,i}-\tilde{P}_{w,i}-\tilde{P}_{pv,i}-\sum_{j=1}^{M}P_{th,j}(i)-P_{ES}(i)=0\right\}\ge\alpha \tag{28}$$

The plausibility chance constraint for the rotating standby constraint can be expressed as follows:

$$Cr\left\{\tilde{P}_{load,i}-\tilde{P}_{w,i}-\tilde{P}_{pv,i}-\sum_{j=1}^{M}P_{th,j}(i)-P_{ES}(i)\le 0\right\}\ge\alpha \tag{29}$$

It should be noted that the rotating standby constraint of the system deals with the uncertainty of the predicted values, so in deterministic scheduling problems, it is usually necessary to include a standby power P_i, whereas with the fuzzy parameter dealing with the predicted values, the uncertainty of the predicted values has already been dealt with in the constraints, and thus there is no need to set a separate standby power. Using the clear equivalence classes under the trapezoidal fuzzy parameters, the clear equivalence classes for the power balance constraint and the rotating standby constraint are, respectively:

$$\begin{aligned}&(2-2\alpha)(P_{\text{load},i3}-P_{\text{w},i2}-P_{\text{pv},i2})\\&+(2\alpha-1)(P_{\text{load},i4}-P_{\text{w},i1}-P_{\text{pv},i1})\\&-\sum_{j=1}^{M}P_{\text{th},j}(i)-P_{\text{ES}}(i)=0\end{aligned} \tag{30}$$

$$\begin{aligned}&(2-2\alpha)(P_{\text{load},i3}-P_{\text{w},i2}-P_{\text{pv},i2})\\&+(2\alpha-1)(P_{\text{load},i4}-P_{\text{w},i1}-P_{\text{pv},i1})\\&-\sum_{j=1}^{M}P_{\text{th},j}(i)-P_{\text{ES}}(i)\le 0\end{aligned} \tag{31}$$

Here, $P_{w,i1}, P_{w,i2}$ - wind power affiliation parameter; $P_{pv,i1}, P_{pv,i2}$ - photovoltaic affiliation parameter; $P_{load,i3}, P_{load,i4}$ - load affiliation parameters.

When calculating the new energy penalty cost, because the fuzzy parameters can not be directly applied in the formula calculation, use equation (30) and (31) to equate the output of wind power and photovoltaic in the time period of i:

$$\tilde{P}_{w,i}=\frac{1-\alpha}{2}(P_{w,i1}+P_{w,i2})+\frac{\alpha}{2}(P_{w,i3}+P_{w,i4}) \tag{32}$$

$$\tilde{P}_{pv,i}=\frac{1-\alpha}{2}(P_{pv,i1}+P_{pv,i2})+\frac{\alpha}{2}(P_{pv,i3}+P_{pv,i4}) \tag{33}$$

Then the wind and light abandonment in i time period can be expressed as:

$$P_{w,p}(i)=P_{w,fc}(i)-\tilde{P}_{w,i} \tag{34}$$

$$P_{pv,p}(i)=P_{pv,fc}(i)-\tilde{P}_{pv,i} \tag{35}$$

Here, $P_{w,fc}(i),P_{pv,fc}(i)$ - the predicted value of wind and PV output at the moment of i, MW.

III. C. Model solving for improved hybrid gray wolf algorithm

III. C. 1) Gray Wolf Optimization Algorithm

Gray Wolf Optimization (GWO) algorithm. According to the hierarchy within the wolf pack, the wolf pack is divided into four different identities such as α,β,δ and ω, among which α wolves, β wolves and δ wolves are the head wolves, and α wolves have the highest rank, which is called the optimal individual; β wolf is second in rank to the α wolf and is a suboptimal individual in the population; δ wolf is lower in rank than the α wolf and the β wolf, but higher than the ω wolf, and is a leader in the third tier of the population. The ω wolf has the lowest rank and needs to accept the leadership of 3 kinds of head wolves [17]. The wolves form an encirclement to encircle the prey after constant wandering, and finally capture the prey by constantly contracting the encirclement.

(1) The following formula is used to update the position of the wolf pack during the process of encircling the prey as follows:

$$\begin{cases}D=|C\times X_p(k)-X(k)|\\C=2\times r_2\end{cases} \tag{36}$$

$$\begin{cases}X(k+1)=X_p(k)-A\times D\\A=2\times a\times r_1-a\end{cases} \tag{37}$$

In Eq. (36)~Eq. (37): k is the number of evolutionary generations; $X_p(k)$ is the position of the prey when the number of evolutionary generations is k; $X(k)$ is the position of the gray wolf when the number of evolutionary generations is k, and r_1,r_2 are the random numbers in the range of [0, 1]; a is the contraction coefficient; C,A are the positional parameter; D is the distance of the prey from the gray wolf.

(2) The GWO algorithm uses the positions of the three head wolves to determine the location of the prey, and the other individual gray wolves update their positions according to the positions of the three head wolves to surround the prey, and the mathematical model of this process is:

$$\begin{cases}D_\alpha=|C_1\times X_\alpha(k)-X(k)|\\D_\beta=|C_2\times X_\beta(k)-X(k)|\\D_\delta=|C_3\times X_\delta(k)-X(k)|\end{cases} \tag{38}$$

$$\begin{cases}X_1=X_\alpha(k)-A_1\times D_\alpha\\X_2=X_\beta(k)-A_2\times D_\beta\\X_3=X_\delta(k)-A_3\times D_\delta\end{cases} \tag{39}$$

$$X(k+1)=\frac{X_1+X_2+X_3}{3} \tag{40}$$

In Eq. (38)~Eq. (40): $D_\alpha,D_\alpha,D_\beta,D_\delta$ are, in order, the prey's distance from the α,β,δ wolf; $X_\alpha(k),X_\beta(k)$ in order of the position of the α,β,δ wolf when the evolutionary algebra is k; X_1,X_2,X_3 in order of the distance of the ω wolf from the α,β,δ wolf.

(3) The expression for the contraction coefficient a is:

$$a=2-2\times\frac{k}{k_{\max}} \tag{41}$$

where $k_{\max}$ is the upper limit of the evolutionary algebra.

III. C. 2) Improvement of the GWO algorithm

The GWO algorithm is simple in principle and effective in global search, but it may stagnate when performing local search, thus falling into the local optimum. Aiming at this shortcoming, the article introduces the idea of differential evolution in the GWO algorithm, and uses the operations of crossover, mutation and selection of the differential evolution algorithm to make the algorithm jump out of the local optimum in time, and obtains the HGWO algorithm.

(1) The mutation operation process is as follows:

$$v_i(k) = x_{r_4}(k) + w \times (x_{r_5}(k) - x_{r_6}(k)) \tag{42}$$

Here, $v_i(k)$ is the i th mutated individual at k evolutionary generations; r_4, r_5, r_6 all denote integers; $x_{r4}(k), x_{rs}(k), x_{r6}(k)$ are all unmutated individuals; w is the coefficient of variation. mutated individuals; w is the coefficient of variation.

(2) After obtaining mutated individuals, crossover operations can be performed on mutated and unmutated individuals to obtain new individuals to increase the diversity of gray wolves as follows:

$$z_i(k) = \begin{cases} v_i(k) & rand < p_i \\ x_i(k) & rand > p_i \end{cases} \tag{43}$$

Here, $z_i(k)$ is the new individual produced when the number of evolutionary generations is k; p_i is the selection probability; rand is a random number in the range of [0, 1]; and $x_i(k)$ is the unmutated individual.

(3) Selection operations are performed on new individuals and parents to obtain individuals with better fitness values as follows:

$$x_i(k+1) = \begin{cases} z_i(k) & f(z_i(k)) < f(x_i(k)) \\ x_i(k) & f(z_i(k)) > f(x_i(k)) \end{cases} \tag{44}$$

Here, $f(z_i(k))$ is the fitness value of individual $z_i(k)$; $f(x_i(k))$ is the fitness value of individual $x_i(k)$.

(4) Whether to perform the differential evolution operation depends on the selection probability, which is expressed as:

$$p_i = \frac{f(x_i)}{\sum_{i=1}^{N} f(x_i)} \tag{45}$$

Here, $f(x_i)$ is the fitness value of individual gray wolf x_i; N is the number of gray wolves.

III. C. 3) Model solving

In order to realize the economic operation of VPP, the article adopts the hybrid gray wolf algorithm to solve the VPP economic dispatch model, and the solution process of HGWO algorithm is as follows:

(1)Set the VPP operation parameters, each equipment operation constraints and scheduling period, the VPP operation parameters mainly include each equipment output situation, equipment operation parameters, load demand and interruptible load, and so on.

(2) Initialize the gray wolf population and set the HGWO parameters, which mainly include the number of gray wolves, selection probability, and upper limit of evolutionary generations.

(3) Take the minimization of VPP operation cost as the search objective of the HGWO algorithm, use the objective function Eq. (1) to calculate the value of individual adaptation of gray wolves, and determine the α wolf β wolf, δ wolf, and ω wolf in the population by comparison;

(4) Calculate the selection probability p_i according to Eq. (45), and update the gray wolf position using Eq. (38) to Eq. (40) if $p_i \geq rand$ is satisfied, otherwise, update the gray wolf position using Eq. (42) to Eq. (44).

(5) Determine whether the current number of iterations reaches the pre-set upper limit value, if yes, the current optimal solution is obtained, i.e., it is the minimum operating cost of VPP; if not, the program returns to the previous step.

IV. Analysis of examples

IV. A. Optimal Scheduling Tests of Virtual Power Plant Loads under Source-Load Uncertainty

IV. A. 1) Parameterization of the virtual power plant structure

A virtual power plant is established in the simulation software, with the following components: 120MW photovoltaic power plant, 40MW electric boiler and 210MW wind farm. The heat price of the virtual power plant and the standard coal price is 100 Yuan/MWh, 493 Yuan/t. The ratio factor of electricity traded with the grid is 0.05. The hourly

operation and maintenance cost of the wind farm and the photovoltaic power plant is 12 Yuan/MW, 23 Yuan/MW, respectively, and the relative errors of the two source-load predictions are 11% and 6%. If the electric boiler is a 10kV electrode hot water boiler, its electric heat conversion efficiency is more than 99%. According to the characteristics of source-load uncertainty, the parameter values set the relevant load information as shown in Table 1.

Table 1: Load parameter information

Parameter name	Numerical value
Interrupt section/MW	[0,11]
Excitation section/MW	[0,8]
Interruptible standby compensation coefficient	0.5
Unit scheduling cost coefficient	0.89
Incentive backup compensation coefficient	0.37
Price discount rate/%	0.77

Let the real demand of the load be equal to the source-load forecast value of the day-ahead, then the load demand as well as the day-ahead tariff situation are shown in Fig. 2, respectively.

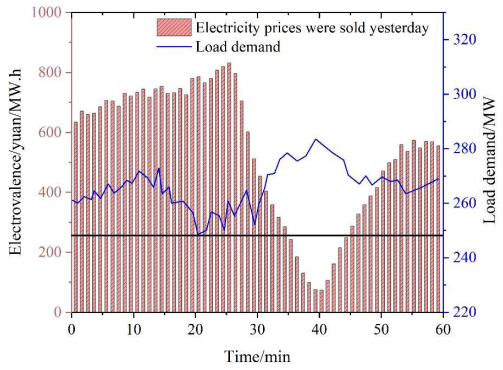

Figure 2: The load requirement of the virtual power plant is a schematic of the last price

IV. A. 2) Analysis of the effect of optimal scheduling of loads in virtual power plants

Under the precondition that the confidence level of the rotating standby reliability opportunity constraint of the virtual power plant is 1, the simulation software is used to plot the changes in the next day's output estimates for different optimal dispatch strategies under multiple markets, under demand response, and under the source load uncertainty in this paper, as shown in Fig. 3.

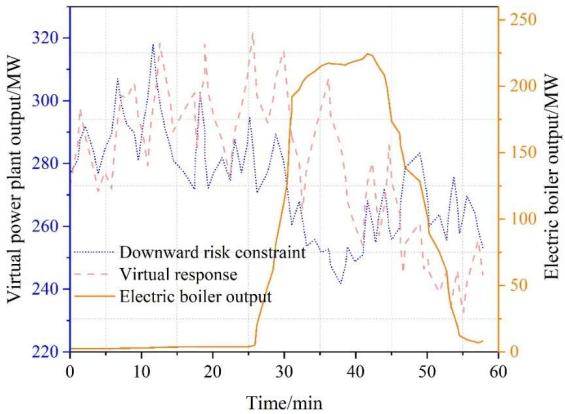

Figure 3: The next day of the virtual power plant is estimated to be the output of the electric boiler

After combining the power curve in the previous section with the trend of the electricity price in the previous day, it can be seen that: the method in this paper is based on the source-load uncertainty of the normal distribution, and

through the curtailment of the power and load probability distribution model, combined with the optimal scheduling objectives of energy consumption and operation cost, in the low electricity price interval, in order to achieve the purpose of stop-loss, the power of the virtual plant is adjusted downward, so that the maximum power of the electric boiler is exactly the minimum load demand of the virtual power plant (that is, 249 MW); in the high electricity price interval, the heat supply of the electric boiler is greatly reduced to increase the revenue. 249 MW); in the high electricity price range, the output is greatly increased and, at the same time, the heat supply of the electric boiler is greatly reduced to increase the revenue. However, the comparison method does not make effective real-time scheduling in response to changing trends in electricity prices, resulting in additional energy consumption by the virtual power plant.

The schematic diagram of the reserved rotating reserve capacity a few days ago is shown in Fig. 4. Combining the rotating reserve capacity of each optimal scheduling method shown in Fig. 3, it is found that compared with the GWO method, the method in this paper reserves appropriate positive and negative rotating reserve for the peak and valley zones of the tariff according to the two optimal scheduling objectives of maximizing the amount of energy consumed and minimizing the operating cost. In the peak-valley zone of the tariff, the method utilizes less negative spinning reserve capacity and more positive spinning reserve capacity to reduce the output of the power plant and solve the problem of insufficient output of wind farms and photovoltaic plants; in the peak-peak zone of the tariff, the method also increases the output and obtains the revenue by appropriately reserving the positive and negative spinning reserve capacity; in terms of spinning reserve capacity of interruptible and incentive customers, the method adopts the following method: (1) the power plant and flexible loads are dispatched by the method, (2) the power plant is dispatched by the method, and (3) the power plant and flexible loads are dispatched by the method. For the spinning reserve capacity of the dispatching plant and the flexible loads, the positive spinning reserve capacity for the high tariff band is shared by the flexible interruptible load users to increase the output; for the negative spinning reserve capacity for the low tariff band, the flexible incentive load users are used to reduce the output loss.

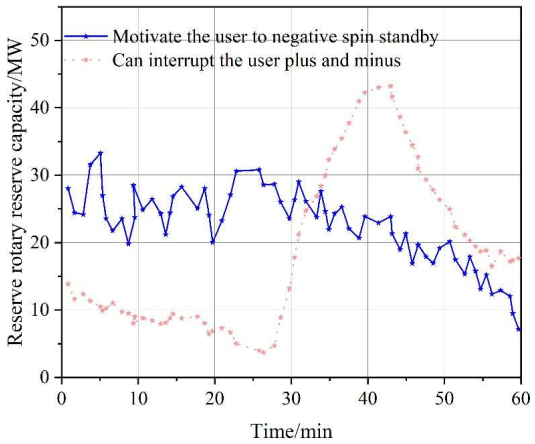

Figure 4: Reserved rotary reserve capacity

From the perspective of economic benefits of different optimization scheduling methods, the optimization scheduling effect of loads is analyzed objectively, as shown in Figure 5. According to the values of the three indexes in the figure, the expected purchasing capital (A1), the expected selling capital (B1) and the overall expected benefit (H1), it can be seen that after the optimization of scheduling in this paper, the cost of increasing the price of electricity in order to buy and the cost of decreasing the price of electricity in order to sell are more desirable than that of the GWO method, and the larger expected benefit indexes further validate that the method can achieve high economic efficiency, which has certain reliability and feasibility. The large expected benefit index further verifies that the method can achieve high economic efficiency and has a certain degree of reliability and feasibility.

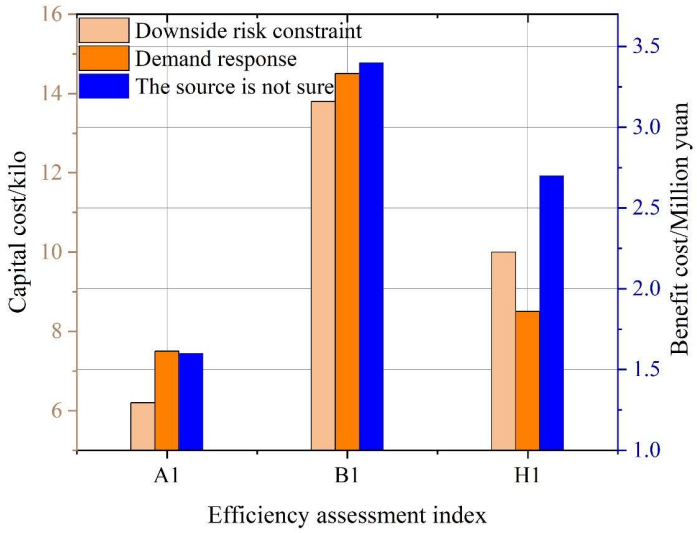

Figure 5: Economic performance indicator schematic

IV. B. Simulation and Analysis of Demand Response with Different Load Participation

IV. B. 1) Description of example parameters

The VPP consists of 1×2MW gas turbine; 2×2MW wind power plant as well as energy storage and customer load. The maximum output of the gas turbine is 2MW; the parameters of energy storage are shown in Table 2; Table 3 shows the time-sharing tariff table formulated by the VPP dispatch center, and Figure 6 shows the wind power and load output curves. The auto-elasticity coefficient of price demand response is taken as -0.2, cross elasticity coefficient is 0.03.MATLAB toolkit is used to solve the model.

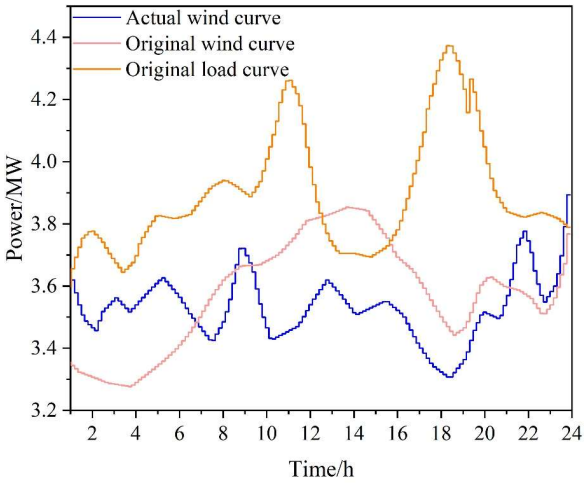

Figure 6: Wind power and user load curve

Table 2: Storage battery parameters

Maximum charging power /MW	Minimum storage energy/MW h	Maximum storage energy/MW h	Charge discharge/(yuan MW/h-1)
2	1	3	Market price

Table 3: Hourly tariff meter

Peak valley	Time period	Electrovalence (yuan/k W·h)-1
Peak	7:00-8:00,11:00-14:00,18:00-21:00	0.5578
Flat	8:00-11:00,14:00-18:00,21:00-23:00	0.5158
Valley	23:00- The next day 7:00	0.3179

The day-ahead and real-time tariff curves are shown in Figure 7.

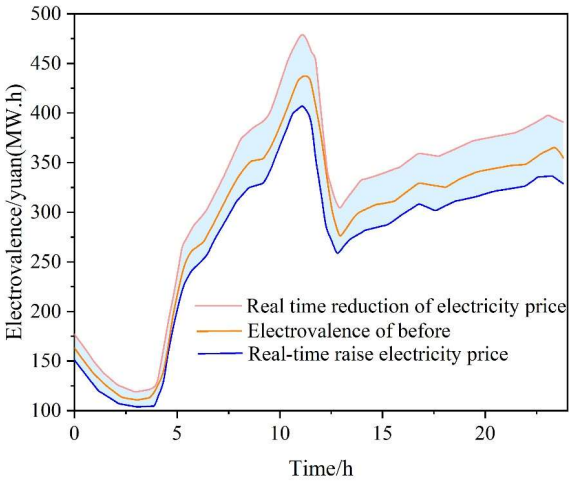

Figure 7: Current and real-time market price curve

IV. B. 2) Analysis of simulation results

1) Simulation and analysis of different loads participating in demand response

Consumers and VPPs are regarded as equally important subjects of interest, and are analyzed in the actual scheduling considering that users and VPPs occupy the same position.

Scenario 1: Customers do not participate in demand response.

Scenario 2: Only Class I and II loads participate in price demand response.

Scenario 3: Only Class III loads participate in incentive demand response.

Scenario 4: Class I, II, and III loads participate in demand response at the same time.

The comparison of the actual benefits of virtual power plants under different scenarios is shown in Table 4. As can be seen from the table, the VPP gain is minimized when the user does not participate in DR, and the VPP gain is maximized when the user 3 loads participate in DR at the same time, the VPP output meets the load demand and there is part of the processing sold to the electricity market.

Table 4: Comparison of actual earnings of virtual power plants

Scene	Earnings/yuan	Unit cost/yuan	User compensation /yuan	Market transaction /yuan
Scene 1	172693.216	240.1075	0	-4592.941
Scene 2	251514.1	212.3707	0	-4216.0485
Scene 3	250944.05	231.0767	14784.235	1146.2725
Scene 4	251515.3	199.2111	4986.22	3382.804

2) The state of VPP energy storage device and gas turbine output curve when the load is finely engaged in demand response.

The state of energy storage charging and discharging and the gas turbine output curve are shown in Fig. 8. From the figure, it can be seen that when the output before VPP day is greater than the actual output, the energy storage absorbs a small amount of power at this time, such as at 6 o'clock when the storage device is in the state of energy storage; when the VPP day is less than the actual output, due to the peak transfer of a portion of the load volume, the storage device is in the discharging state, such as at 18 o'clock.

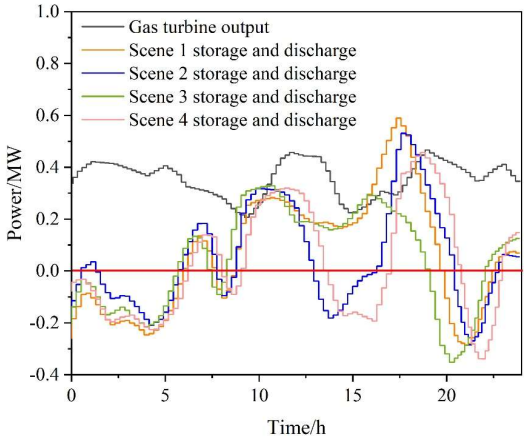

Figure 8: Energy storage and discharge state and gas turbine output curve

3) Load profiles for refined categorization of participation in demand response

The demand response load curves for different scenarios are shown in Fig. 9. From the figure, it can be seen that the peak-to-valley difference of the load curves participating in DR its curves after the load refinement are all reduced. Scenario 1 has a better valley filling effect; Scenario 2 has a better peak shaving effect; and Scenario 3 has a smoother load curve. The cost of electricity consumption of customers under different scenarios is shown in Table 5. It can be seen that when the three types of loads participate in DR at the same time, it shows that the load refinement can promote the user demand response and the user's electricity consumption cost is minimized.

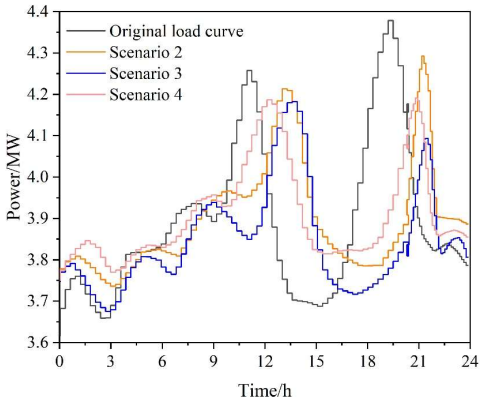

Figure 9: Demand response load curve of different scenarios

Table 5: User use of electricity for different scenarios

Scene	Power cost (yuan)
Scenario 1	40753.25
Scenario 2	40584.5842
Scenario 3	39876.1137
Scenario 4	38972.1096

4) VPP unbalanced output analysis

As the actual wind power output and the planned output deviation, in the VPP on the load refinement of the participation of DR and energy storage device charging and discharging to compensate for the deviation, if there is still a deviation, i.e., for the unbalanced output, the VPP imbalance in three scenarios as shown in Figure 10.

In the figure, the output above the axis is positive on behalf of the VPP power market sales, and below the axis is the VPP power purchase from the power market. As can be seen from the figure, when class I and II loads participate in price demand response through the transfer of load volume, the load volume of the VPP insufficient output period is transferred to the period of more output; by interrupting a part of class III loads to reduce the

imbalance output, and the three types of loads participate in DR at the same time, the VPP imbalance output is minimized.

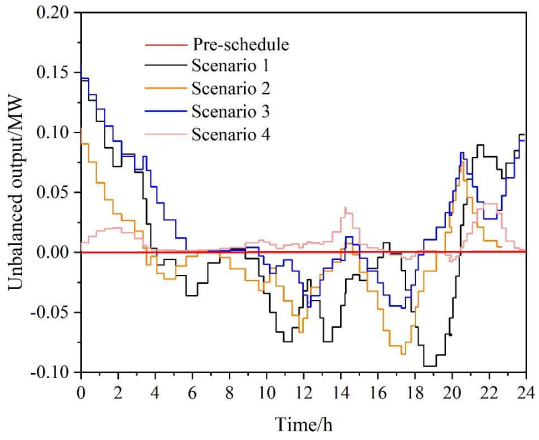

Figure 10: VPP unbalanced output

V. Conclusion

The virtual power plant economic optimization scheduling model is established with the objective function of minimizing the total cost of VPP operation cost. The differential evolution idea is introduced into the GWO algorithm, and the differential evolution strategy is used to make the algorithm jump out of the local optimum in time to obtain the HGWO algorithm, and simulation experiments are carried out. The experimental results show that the HGWO algorithm has a better regulation of the peak-trough of the electricity price, and can achieve economic benefits with reliability. From the comparison of the state of VPP energy storage device, load curve, user electricity cost and VPP unbalanced output, it can be seen that the price demand response fills the valley with stronger ability, the peak shaving ability of incentive demand response is stronger, the peak-valley difference of the load curve of the three types of loads participating in demand response at the same time is minimized, the VPP gain is maximized, and the user electricity cost is minimized, and a win-win situation for the VPP and the user is realized.

Funding

This research was supported by the Dynamic quantitative measurement of dust removal system based on fuzzy neural network (Heng20240006).

References

[1] Reihani, E., Motalleb, M., Ghorbani, R., & Saoud, L. S. (2016). Load peak shaving and power smoothing of a distribution grid with high renewable energy penetration. Renewable energy, 86, 1372-1379.

[2] Uddin, M., Romlie, M. F., Abdullah, M. F., Abd Halim, S., Bakar, A. H. A., & Kwang, T. C. (2018). A review on peak load shaving strategies. Renewable and Sustainable Energy Reviews, 82, 3323-3332.

[3] Manojkumar, R., Kumar, C., Ganguly, S., & Catalão, J. P. (2021). Optimal peak shaving control using dynamic demand and feed-in limits for grid-connected PV sources with batteries. IEEE Systems Journal, 15(4), 5560-5570.

[4] Delavari, A., & Kamwa, I. (2017). Demand-side contribution to power system frequency regulation:-a critical review on decentralized strategies. International Journal of Emerging Electric Power Systems, 18(3), 20160237.

[5] Han, Y., & Lin, X. (2024). Multi-demand-side resource regulation capacity assessment for distribution network safety and security. Journal of Computational Methods in Science and Engineering, 24(4-5), 2267-2282.

[6] Liu, J., Samson, S. Y., Hu, H., Zhao, J., & Trinh, H. M. (2022). Demand-side regulation provision of virtual power plants consisting of interconnected microgrids through double-stage double-layer optimization. IEEE Transactions on Smart Grid, 14(3), 1946-1957.

[7] Mao, T., Guo, X., Xie, P., Zhou, J., Zhou, B., Han, S., ... & Sun, L. (2020, November). Virtual power plant platforms and their applications in practice: a brief review. In 2020 IEEE Sustainable Power and Energy Conference (iSPEC) (pp. 2071-2076). IEEE.

[8] Dall'Anese, E., Guggilam, S. S., Simonetto, A., Chen, Y. C., & Dhople, S. V. (2017). Optimal regulation of virtual power plants. IEEE transactions on power systems, 33(2), 1868-1881.

[9] Wang, Z., Wang, Y., Xie, L., Pang, D., Shi, H., & Zheng, H. (2024). Load Frequency Control of Multiarea Power Systems with Virtual Power Plants. Energies, 17(15), 3687.

[10] Golpîra, H., & Marinescu, B. (2024). Enhanced frequency regulation scheme: An online paradigm for dynamic virtual power plant integration. IEEE Transactions on Power Systems.

[11] Wang, K., Cheng, B., Ren, Y., Wang, S., Ji, R., & Kong, X. (2023). Flexible resource dynamic aggregation regulation method of virtual power plant to ensure more renewable energy generation. Process Safety and Environmental Protection, 180, 339-350.

[12] Oshnoei, A., Kheradmandi, M., Blaabjerg, F., Hatziargyriou, N. D., Muyeen, S. M., & Anvari-Moghaddam, A. (2022). Coordinated control scheme for provision of frequency regulation service by virtual power plants. Applied Energy, 325, 119734.

[13] Yavuz, L., Önen, A., Muyeen, S. M., & Kamwa, I. (2019). Transformation of microgrid to virtual power plant–a comprehensive review. IET generation, transmission & distribution, 13(11), 1994-2005.
[14] Sun, X., Xie, H., Qiu, D., Xiao, Y., Bie, Z., & Strbac, G. (2023). Decentralized frequency regulation service provision for virtual power plants: A best response potential game approach. Applied Energy, 352, 121987.
[15] Björk, J., Johansson, K. H., & Dörfler, F. (2022). Dynamic virtual power plant design for fast frequency reserves: Coordinating hydro and wind. IEEE Transactions on Control of Network Systems, 10(3), 1266-1278.
[16] Zuo, J., Xu, C., Ji, Y., Wang, W., Ma, S., & Zhang, Y. (2024, October). Investigating the Bidding Strategy of Loaded Virtual Power Plant While Considering Multiple Demand Response Resources. In 2024 IEEE PES 16th Asia-Pacific Power and Energy Engineering Conference (APPEEC) (pp. 1-4). IEEE.
[17] Deepshikha Kumari,Prashant Pranav,Abhinav Sinha & Sandip Dutta. (2025). A hybrid cheetah and grey wolf optimization algorithm for network intrusion detection. Engineering Research Express,7(1),015256-015256.